emerald PUBLISHING

Rapid Prototyping Journal

Proof of Concept of a Novel Combined Consolidation and Transfer Mechanism for Electrophotographic 3D Printing

Journal:	*Rapid Prototyping Journal*
Manuscript ID	RPJ-04-2018-0111
Manuscript Type:	Original Article
Keywords:	Electrophotography, Layered manufacturing, Laser printing, 3D Printing, Solid freeform fabrication

Abstract

Purpose: This paper develops and then evaluates a novel consolidation and powder transfer mechanism for electrophotographic 3D printing, designed to overcome two longstanding limitations of electrophotographic 3D printing: fringing and a build height limitation.

Design/methodology/approach: Analysis of the electric field generated within electrophotographic printing was used to identify the underlying causes of the fringing and build height limitations. A prototype machine was then designed and manufactured to overcome these limitations, and a number of print runs carried out as proof of concept studies.

Findings: The analysis suggested that a machine design which separated the electrostatic powder deposition of the print engine from the layer transfer and consolidation steps is required to overcome fringing and build height limitations. A machine with this build architecture was developed and proof of concept studies showed that the build height and fringing effects were no longer evident.

Research limitations/implications: Electrophotography was initially seen as a promising technology for 3D printing, largely because the potential for multi-material printing at high speed. As these limitations can now be overcome, there is still potential for electrophotography to deliver a high speed 3D printing system which can build parts consisting of multiple materials.

Originality/value: The analysis of electrophotography, the new method for the transfer and consolidation of layers and the proof of concept study are all original, and provide new information on how electrophotography can be adopted for 3D printing.

1. Introduction

Electrophotography (EP) is the base technology for both photocopiers and laser printers, in which a latent electrostatic image is developed by a toner powder and subsequently transferred and fixed on to print media. The EP process is dependent on the physical properties of an organic photoconductor (OPC), which maintains a surface charge in the absence of light and conversely conducts and discharges when light is present. This property allows the selective discharging of portions the charged OPC by, in the case of a laser printer, the digital modulation of an incident laser or light emitting diode (LED) array. EP powder image formation is a six step process, all of which are performed at the heart of a laser printer in a single print engine assembly (Figure 1).

The six steps are:

Photoconductor Cleaning: The OPC is exposed to a uniform light source, often an LED array, allowing residual charge to pass to ground before being wiped free of toner residue.

Photoconductor Charging: In the absence of light the surface of the photoconductor is charged by contact with a charge roller at elevated potential, or a corona discharge type device.

Imaging: The charged surface of the photoconductor is exposed selectively to an appropriate wavelength of light resulting in the formation of a latent electrostatic image.

Powder Development: The latent electrostatic image is developed with an electrostatically charge toner powder brought into close proximity.

Image Transfer: The developed powder image is electrostatically transferred on to a printing medium such as paper.

Image Fixing: The transferred image is thermally bound to the substrate often through the use of heated rollers.

There are a number of subtly different techniques to achieve powder development and at the highest level these can be divided into two development subgroups, distinct by the number of materials present within the toner powder, mono component development (MCD) and dual component development (DCD). MCD strategies rely on the triboelectric charging characteristics of toner particles, contained within a mechanical agitated cartridge, to produce and hold a uniform powder layer on a developer roller. The thickness of this powder layer, typically tens of microns thick (Pai and Springett, 1993), is metered by a doctor blade and in many embodiments it is this powder layer which separates the spring mounted developer roller from the OPC during image development. DCD type systems, as the name suggests, employ two materials within a mechanically agitated cartridge. As in the MCD systems, the toner particles tribocharge and instead of coating the developer roller directly, the particles electrostatically adhere to the surface of magnetic carrier beads which then go on to adhere to the surface of a developer roller. The magnetic carrier beads are typically an order of magnitude larger than the toner particles (Schein, 2013), as shown in Figure 2.

In the DCD system, the developer roller rotates around a number of coaxial stationary magnets which produce a ‘magnetic brush’ effect as the magnetic carrier beads line up with the magnetic

field lines of the stationary magnets (Kawamoto et al, 2016). Frictional forces rotate the brush past the OPC at which point the image is developed by toner exchange from the carrier beads to the OPC. This exchange occurs due a relatively weak electrostatic force holding the toner in contact with the carrier bead and a stronger electric field of the undeveloped image present on the OPC. The carrier beads are then recycled back into the cartridge where they pick up a fresh toner layer and the process is repeated. To allow for the passing of the magnetic brush between developer roller and OPC, the developer roller must be mounted several hundred microns, or more, from the OPC. The schematic in Figure 3 shows the comparative working principles of MCD and DCD, and illustrates the relative displacement of developer roller to OPC in each system.

Over the past two decades a range of additive manufacture and 3D printing systems have emerged and have become a significant subset of manufacturing processes (Wong and Hernandez, 2012). The low cost and reliability of laser printing systems has seen a number of researchers investigate the potential for adopting an electrophotographic approach for 3D printing (Kumar and Zhang, 1999; Kumar and Dutta, 2003, 2004; Kumar et al, 2004; Cormier et al, 2000, 2002; Banerjee, 2006, 2008; Wimpenny et al, 2009; Jones et al, 2010) and a number of patents disclosed (Bynum, 1992; Grender, 1994, 2001; Kumar, 2000; Wimpenny & Banerjee, 2008). Research undertaken by Kumar and Dutta (2003) identified a build height limitation when using an electric field source located at the base of a build platform and demonstrated that while charging the build surface between deposited layers increased build height, it also caused unwanted material to be deposited across the build platform. The height of parts in the initial stages of Kumar's work was 1-2mm with a later paper (Kumar & Dutta 2004) claiming parts up to 3mm, but with significant fringe build up due to the non-uniform electric field distribution across the build surface. Kumar concluded that this fringe build up could be minimised with a co-printed support material. Other research has focused on the possibility of printing functional materials by EP. Cormier (2000) successfully printed high density polyethylene (HDPE) from a standard laser printer as well as experimenting with standard styrene based toners in multiple colours. Cormier noted that during colour printing the density of the toner layers at the interface between colours was appreciably higher than towards the centre of a mono print (Cormier et al, 2002). Following on from Cormier's work, Wimpenny (2008) successfully printed a number of additional engineering materials; polypropylene (PP), low density polyethylene (LDPE), polyvinyl acetate (PVA) and a Polybutylene Terephthalate (PBT). Bynum's patent of 1992 is distinct from other works in that it discloses a method of EP which relies on electric fields only for image development and transfer onto a belt. The transfer of layers onto the build platform is performed mechanically in a multi-step process whereby a layer is tackifed and then physically transferred through the application of pressure from a press stage and large backup plate.

In summary, previous work on electrophotographic 3D printing demonstrated that the technique could be successfully applied to a range of polymer materials, but identified a build height limitation and a fringing effect. The research presented in this paper develops and evaluates a machine design which overcomes those two limitations. In order to understand why these effects occurred, models of the electrostatic field were developed and are presented in the next section prior to the description of the prototype machine and test builds produced.

2. Electrostatic Field Modelling

The powder development process begins with the formation of an electrostatic image on the surface of an organic photoconductor (OPC). An OPC consists of multiple layers bound to a conductive tube or flexible belt substrate. The composite structure of the most commonly used OPC is shown in Figure 4. On the surface of the charge transport layer (CTL), prior to exposure, a negative charge is applied. Exposure to light causes the charge generation layer (CGL) to produce a positive charge, which is then 'transported' through the CTL to neutralise the area directly above the point of CGL exposure. This process leaves a charged image on the surface of the CTL which interacts with the relative contrasting polarity present on the substrate, resulting in an electric field. The majority of this electric field is contained within the OPC layers, with only the edges of the latent image producing a field above the OPC (Weiss, 2010). As it is this field that is ultimately responsible for the deposition pattern and density of powder upon the OPC surface during development, the lack of field towards the centre of the latent image relative to the edge produces developed images with significant fringing, as illustrated in Figure 5.

The developer roller contained within an MCD EP print engine is designed to feed a metered layer of toner to the OPC for the purposes of image development. Developer rollers in modern EP engines have a dual purpose, also acting as a developer electrode. This electrode interacts with the charge present on the surface of the CTL, generating a development field above the OPC. For a uniform field, the electrode should ideally be placed in close proximity to the OPC surface at the same voltage and dielectric displacement as the equivalent combined dielectric thickness of the CTL, CGL and undercoat layer (UCL). Figure 6 is a representative schematic of a developer electrode displaced from the surface of an OPC with film thickness *s*, by toner thickness *l*.

In an ideal case where no charge leaked from the surface of an OPC in the absence of light, Pai and Springett (1993) gave the potential *V* across its surface, related to the charge density σ, as

$$\sigma = CV = \frac{\varepsilon_s}{s}V \quad \text{, where } \varepsilon_s = K_s\varepsilon_O \qquad (1)$$

Where C is the geometrical capacitance per unit area of the device and ε_s is the dielectric permittivity of the photoconductor layer of thickness s, K_s is the dielectric constant of the photoconductor material and ε_O is the permittivity of free space. Applying Gauss's law the average electric field E_{ave} above the OPC can be given as

$$E_{ave} = \frac{V_O}{s/K_s + l/K_l} \qquad (2)$$

Where s/K_s is the dielectric thickness of the OPC layers, l/K_l is the dielectric thickness of the toner material between OPC and developer electrode, and V_O is the initial potential on the photoconductor relative to the surface charge density given by equation (1). Assuming OPCs are typically 30 µm in thickness with a dielectric constant of around 3, and depending on the type of developing system, the OPC to electrode displacement can be up to 1500 µm with a dielectric constant of around 4.5 (Weiss, 2010). The relationship between E_{ave} for a given l is shown in Figure 7. The results show that there is an increase in average electric field over the surface of an OPC in the presence of a developer electrode, but offers no insight into the distribution of this charge. To investigate field distribution the OPC and developer electrode system was modelled in QuickField 5.8 (Tera Analysis, USA). The OPC and developer were modelled assuming an OPC thickness of 30µm, a

relative OPC dielectric permeability of 3, a surface charge of 1kV, an OPC to developer relative dielectric permeability of 3 an electrode potential of 0V and an OPC substrate of 0V potential.

The resultant field plot, shown in Figure 8, illustrates a cross section of the field above an OPC with a 2mm wide latent charge on its surface. Figure 8a shows the magnitude and relative X axis position of the applied surface charge. The charge was assumed to be of infinite length perpendicular to the x/y axis presented and is symmetrical about the x axis. Figure 8b shows a model of the system with a 0V potential (developer electrode) over 6mm above the OPC surface, demonstrating the relative field intensity without the influence of the developer electrode. Figure 8c, d, e and f illustrate the effects of a 0V potential developer electrode approaching the surface of the OPC. It is clear from Figures 7 and 8 that both the strength and quality of the electric field present above the surface of the OPC reduce significantly when the developer electrode displacement is increased. As the strength of the electric field dictates the amount of toner powder deposited, the further away the development electrode is from the OPC the more powder will be deposited around the periphery relative to the centre of an image. A DCD system when compared to a MCD system, as discussed previously and as used by other researchers (Kumar and Dutta 2003, 2004; Jones et al, 2010), exacerbates this problem as the developer electrode has to be significantly displaced from the OPC to allow the passage of large magnetic carrier particles. Within an additive manufacturing context this means that if these images with increased fringe powder deposition are stacked to produce a 3D object, the outer wall of the part having more material, will grow faster than the core leading to failed part construction.

We consider that non-uniform electric fields present on OPC and build surface, in addition to the reduction in electric field strength from base generated transfer charges, results in the fringing and build height limitations seen by other researchers.

3. Prototype Machine Design

A number of iterations of an electrophotographic layer manufacturing (EPLM) machine design were required prior to a final prototype design being developed. The final design is presented briefly here, full details of the development process and design iterations can be found in Benning (2011). The prototype EPLM system, a schematic and photograph of which can be seen in figures 9 and 9b, consisted of a ML4500 (Samsung, South Korea) mono-component print engine selected for its low developer electrode / OPC displacement of 15µm - 20µm, a seamless glass fibre reinforced low surface energy PTFE transfer belt, two AC corona charge neutralizers, a cleaning blade, a z-axis, and a coaxially heated transfer and consolidation roller. The system's 6 layer generation steps were controlled by in house developed microprocessor embedded electronics and software.
The 6 steps are:

1. Print data received from slicing software and cached
2. Transfer belt discharged and cleaned
3. Print engine developed powder layer and deposited on to transfer belt
4. Powder image surface discharged
5. The powder image indexed to the build surface where it was held
6. The heated consolidation roller moved across the back of the transfer belt to both thermally transfer the powder image to the build platform and to consolidate the layer to the part under construction, while the peel roller removes the belt from the build platform.

The two key parts of the prototype machine were a mono component print engine and a heated consolidation roller which transferred each layer at elevated temperature in the absence of an electrostatic field. The transfer belt, Figure 10, consisted of a glass fibre reinforced webbing coated on both sides with PTFE.

4. Evaluation of Prototype Machine Performance

The prototype machine was used to make a number of test parts. In the manufacture of these parts the consolidation roller temperature and velocity were set to 180°C and 25mms^{-1} respectively, on the basis of initial testing. The resulting consolidated layers were 5 µm thick. The substrate was a card which had been pre-treated with a tackifying layer through the deposition of three layers without a Z-axis step down. Figure 11 shows a 20 layer (100 µm) part, and Figures 12 & 13 show a 700 layer (3.5 mm high) part. In both cases the build rate was two consolidated layers (10 µm) per minute. The figures show that the fibre reinforcing, shown in Figure 10, left a distinct imprint on the surface of built parts.

Both the 20 layer and 700 layer part illustrate good densification and edge definition, and that the top surface of the part replicates the belt texture and surface finish. The 700 layer part has flaws, but without any evidence of fringing or a build height limitation. The flaws were due to layers 581 to 602 printing incorrectly. The layers in question were not printed in their entirety due to a lack of material present on the developer roller of the laser engine. The printer was paused and the cartridge replaced where upon standard printing and consolidation was resumed. Due to the printing of incomplete layers, the proceeding layers had no underlying support in a number of areas and therefore disparities formed and continued to grow with the artefact. In order to investigate the effectiveness of the consolidation process, the part was removed from the card substrate through the application of heat on the underside of the card. Once released from the card substrate the artefact was bisected using a micro saw. The surface was polished to remove machining marks and showed a fully consolidated and dense structure (Figure 14).

A cross-section view of a fracture surface of the built artefact, as seen in Figure 15, shows evidence of the unsupported bridging of a void within the volume. Damage to the right hand edge is shown in Figure 16.

5. Discussion

5.1 Build Height and Fringing

The results from the multiple layer builds shown in Figures 11-15 we consider to confirm the hypothesis developed from the modelling studies presented in Figure 2, that the fringing and build height constraints observed in previous studies were as a result of non-uniform electric fields present on the surface of the OPC and built artefacts during printing. The prototype machine design presented in section 3 overcomes this limitation and has produced multi-layer parts, going significantly beyond the capabilities of any previously presented electrophotographic additive manufacture system.

Key to achieving this is the effectiveness of the belt and peel roller system in consolidating layers on top of one another. Initially a "backing plate" as described by Bynum (1992) was used, but separating a whole layer from the plate in a single step proved difficult, and the peel roller system was developed as an alternative which progressively deposits the layer onto the build. This was aided by the non-stick (low surface energy) nature of the PTFE belt, which meant that the toner layer preferentially adhered to the build. This means that takification, layer transfer, consolidation and belt removal are combined in one efficient processing step.

5.2 Flaws

The machine developed in this work was proof of concept, and the parts produced contained flaws (as illustrated in Figures 11, 14 and 15) as a result of the system being temporarily starved of powder. Interestingly it was observed that internal flaws could be "bridged", whereas flaws which extended to the periphery of a printed layer could not. We consider that this effect was a result of the printed layer forming a consolidated wafer while still on the belt's surface. The wafer subsequently adhered to the surface of the build platform before the belt was peeled away, as illustrated in Figure 17. Voids which formed on the leading edge of a part being built were unlikely to be bridged, as the layer wafers were unsupported and thus removed by the peeling action of the peel roller.

5.3 Potential for Electrophotographic based 3D Printing

The work presented in this paper has demonstrated that the major limitations in terms of build height and fringing for electrophotographic 3D printing can be overcome. The base technology is widely available and inexpensive, and so the major obstacle to overcome would be productivity. The best productivity obtained by the prototype machine described in section 3 was 4 mm^3/s.

High levels of productivity could only be obtained for a 3D system with a machine design which allowed continuous printing of layers and discrete layer by layer consolidation. One potential way of achieving this would be the use of an accumulator. Figure 18 illustrates this concept, which pays out belt material to the deposition system while consolidation takes place, and then re-accumulates it while the next image is being shuttled into place above the build platform.

For a machine designed such that the print deposition system was the slowest step and assuming; a print speed of 55 mm/s (which is the print speed of the ML4500 print engine used in the prototype machine), a layer width of 200 mm, and a layer thickness of 5 µm, the possible deposition rate would be of the order of 55 mm^3/s. For comparison, commercial SLA systems of comparable resolution, have a deposition rates ranging from 0.2 – 1 mm^3/s (Campbell, et al. 2008), with some lower-cost digital micro-mirror device (DMD) based systems exhibiting deposition rates up to 3.5 mm^3/s with a 10 µm layer thickness (Ember, Autodesk Inc. USA).

6. Conclusions

The work presented in this paper has demonstrated that fringing and build height limitations in electrophotographic 3D printing can be overcome through using a machine design which adopts a monocomponent development system with low developer electrode / OPC displacement, and a design which separates the electrostatic powder deposition of the print engine from the layer transfer and consolidation steps. The novel combination of through belt heating, roller transfer, roller consolidation and belt peeling in one process step demonstrates significant advantage over previous works. The adopted machine architecture allows the powder deposition process to take place under optimal conditions while eliminating unwanted electrostatic effects during transfer and consolidation. Electrophotographic 3D printing has significant potential as a low cost, highly productive 3D printing process.

Acknowledgments

The authors would like to acknowledge the EPSRC and Newcastle University for supporting the work through a PhD Studentship for Benning.

References

Bynum, D.K. (1992). *"Automated Manufacturing System Using Thin Sections",* US Patent 5088047.

Banerjee, S. and Wimpenny, D.I. (2006). *"Laser Printing of Polymeric Materials",* Proceedings of the 17th Solid Freeform Fabrication Symposium, August 14-16, Austin, Texas, pp. 366-374.

Banerjee, S and Wimpenny, D.I. (2008). *"Laser Printing of Soluble Toner for Rapid Manufacturing",* Proceedings from the 2nd International Conference on Additive Technologies, Ptuj, Slovenia, Sept. 17-19.

Benning, M.J. (2011). "*Development of a Novel Electrophotographic Additive Layer Manufacturing Machine",* Newcastle University, https://theses.ncl.ac.uk/dspace/handle/10443/2653.

Campbell, I., Deon de Beer, J.C. & Barnard, L. (2008*). "Stereolithography build time estimation based on volumetric calculations*", Rapid Prototyping Journal, Volume 14, Issue 5, pp. 271 - 279

Cormier, D., Taylor, J., Unnanon, K., Kulkarni, P. & West, H. (2000). *"Experiments In Layered Electro-Photographic Printing",* Proceedings of the 11th Solid Freeform Fabrication Symposium, August 7-9, Austin, Texas, pp. 267 – 274.

Cormier, D., Taylor, J. & West, H. (2002). "*An Investigation of Selective Coloring with 3-D Laser Printing",* Journal of Manufacturing Processes, Volume 4, Issue 2, 2002, pp. 148-152.

Fan, G. (2003). *"Xerography/Electrophotography: The Technology of Photocopiers and Laser Printers",* MAE Dept. Seminar, Clarkson University. https://www.slideshare.net/ffan/xerographyelectrophotography-the-technology-of-photocopiers-and-laser-printers-3748801, accessed 01/05/2018.

Grenda, E. (1994). *"Apparatus of Fabricating 3-Dimensional Objects by Means of Electrophotography, Ionography or similar process",* US Patent Number 6206672.

Horn, T.J. & Harrysson O.L. (2012). *"Overview of current additive manufacturing technologies and selected applications"* Science Progress, Volume 95, Issue 3, pp. 255-282

Jones, J., Wimpenny, D., Gibbons, G. & Sutcliffe, C. (2010). *"Additive Manufacturing by Electrophotography: Challenges and Successes"* In: IS&T's NIP26 and Digital Fabrication 2010, Proceedings of the Conference held in Austin, Texas, 21-24 Sep. 2010.

Kawamoto, H. and Nakayama, N. (2016). "*Overview on Recent Progress in Electrophotography",* Journal of Imaging Science and Technology, Volume 60, Issue 3, pp. 30506-1.

Kumar, A.V. and Zhang, H. (1999). *"Electrophotographic Powder Deposition for Freeform Fabrication",* Proceedings of the 10th Solid Freeform Fabrication Symposium, Austin, Texas, pp 647-654.

Kumar, A.V. (2000). *"Solid Freeform Fabrication using Power Deposition",* US Patent 6066285.

Kumar, A.V. and Dutta, A. (2003). "*Investigation of an Electrophotography Based Rapid Prototyping Technology*", Rapid Prototyping Journal, Volume 9, Issue 2, pp. 95 – 103.

Kumar, A.V. and Dutta, A. (2004). *"Electrophotographic Layered Manufacturing",* Journal of Manufacturing Science and Engineering, Volume 126, pp. 571 - 576.

Kumar, A.V. Dutta, A. & Fay, J.E. (2004). *"Electrophotographic Printing of Part and Binder Powders",* Rapid Prototyping Journal, Volume 10, Issue 1, pp. 7 – 13.

Morita, K., Ikeda, Y. & Tanaka, Y. (2007). *"Organic Photoconductors for Printers",* Fuji Electrical Technical Journal Paper, Volume 53, Issue 2, pp. 58.

Pai, D.M. and Springett, B.E. (1993). *"Physics of Electrophotography",* Reviews of Modern Physics, Volume 65, Issue 1.

Schein, L.B. (2013). *"Electrophotography and Development Physics",* 2nd ed., Springer Science & Business Media.

Thourson, T.L. (1972). *"Xerographic Development processes: A review",* IEEE Transactions on Electron Devices, Volume 19, Issue 4, pp. 495- 511.

Wimpenny D.I. and Banerjee, S. (2008). *"Electrostatic Printing Method and its Use in Rapid Prototyping",* World Patent 2008/096105.

Wimpenny D.I., Banerjee, S. & Jones, J. (2009). "*Laser Printed Elastomeric Parts and Their Properties*" Proceedings of the 20th International Solid Freeform Fabrication Symposium, Austin, Texas, pp 498-506.

Wong, K.V. and Hernandez, A. (2012) *"A Review of Additive Manufacturing"* ISRN Mechanical Engineering, Volume 2012, pp. 1 – 10.

Weiss, D.S. and Abkowitz, M. (2010) *"Advances in Organic Photoconductor Technology",* Chemical Reviews, Vol 110, PP 479 – 526.

Figure Captions

Figure 1 - Schematic of a mono-component laser printing engine

Figure 2 - An SEM image of; (A) toner powder; (B) toner powder electrostatically adhered to a magnetic carrier bead (Fan, 2003)

Figure 3 - Working principles of MCD and DCD

Figure 4 - Illustration of the composite layers of an OPC manufactured to accept negative charge (Morita et al, 2007)

Figure 5 - Illustration of the electrostatic fringing effect generated by weak electric fields in the centre of solid black areas during electrophotographic development (Thourson, 1972)

Figure 6 - Representation of an OPC to developer roller/electrode displacement

Figure 7 - The relationship between the increased displacement of a developer electrode relative to an OPC, l, and the resultant drop in relative average electric field, Eave.

Figure 8 - Finite element visualisations of relative field strength present above an OPC with the charge pattern seen in (a) with: (b) No electrode, (c) An electrode displacement of 1mm, (d) An electrode displacement of 0.5mm, (e) An electrode displacement of 250µm, and (f) An electrode displacement of 85µm.

Figure 9a - The prototype EPLM device

Figure 9b - Prototype test bed

Figure 10 - Surface of the PTFE transfer belt

Figure 11 - An enlarged photograph of the surface of a 20 layer artefact showing no sign of edge fringing

Figure 12 - 700 layer printed cylinder (18.1 mm dia, 3.5 mm high). Layer deposition was from right to left.

Figure 13 - Surface finish and edge definition of a 700 layer artefact.

Figure 14 - A picture of the bisected and polished surface of the 3.5mm artefact showing fully dense consolidation.

Figure 15 - A picture of the fractured surface of a 3.5mm built artefact showing a 1mm long pocket formed between layers which was then bridged by subsequent layers.

Figure 16 - Leading edge defect.

Figure 17 - Mechanism of leading edge defect formation and void bridging

Figure 18 - A sketch of an accumulator system for improved productivity

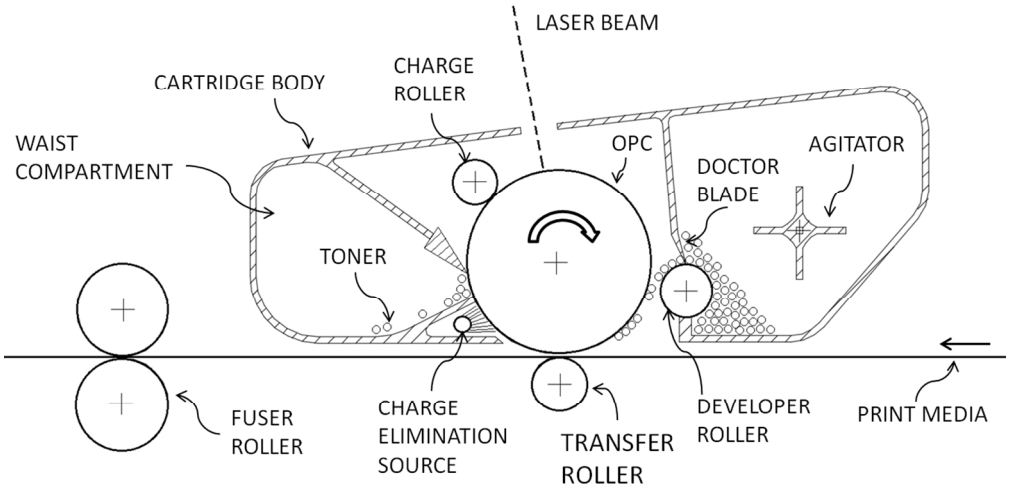

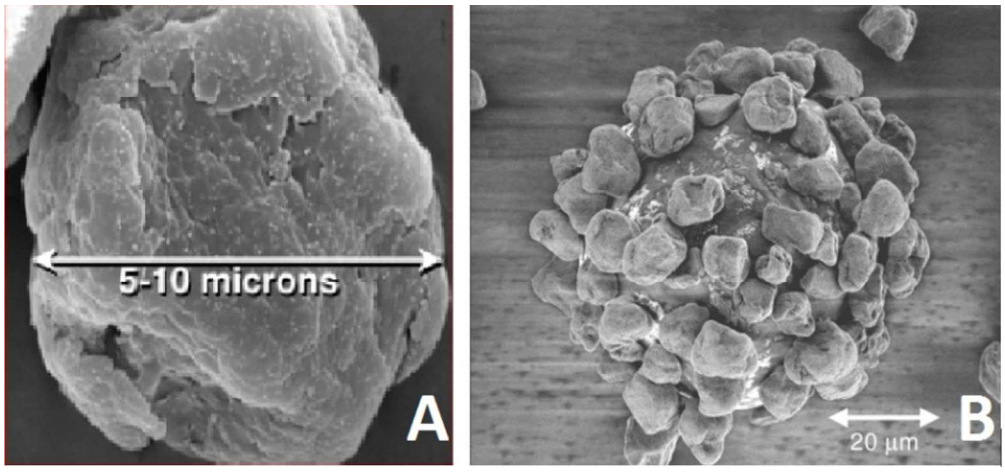

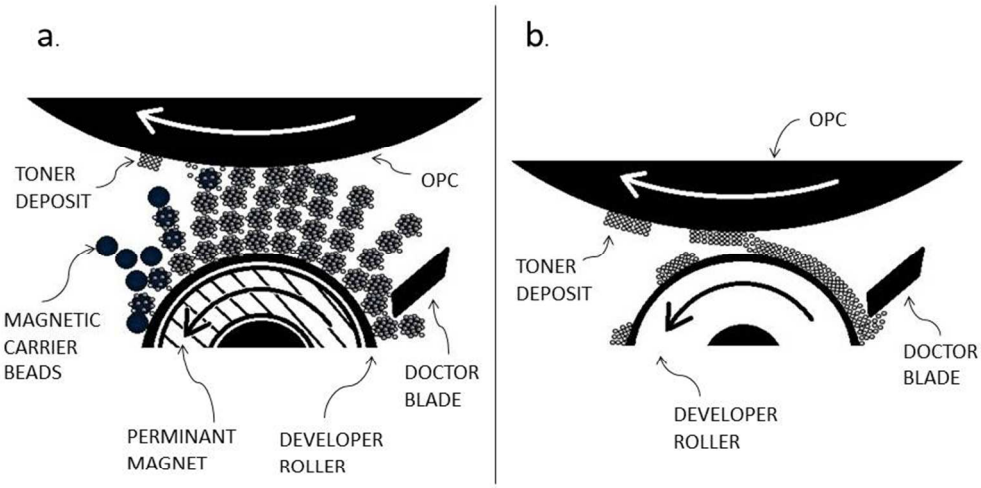

254x190mm (96 x 96 DPI)

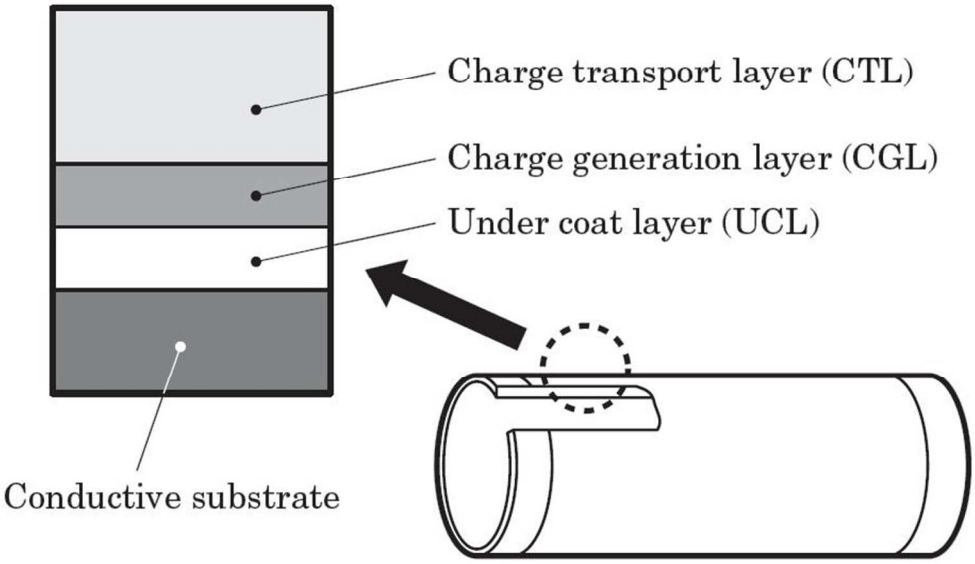

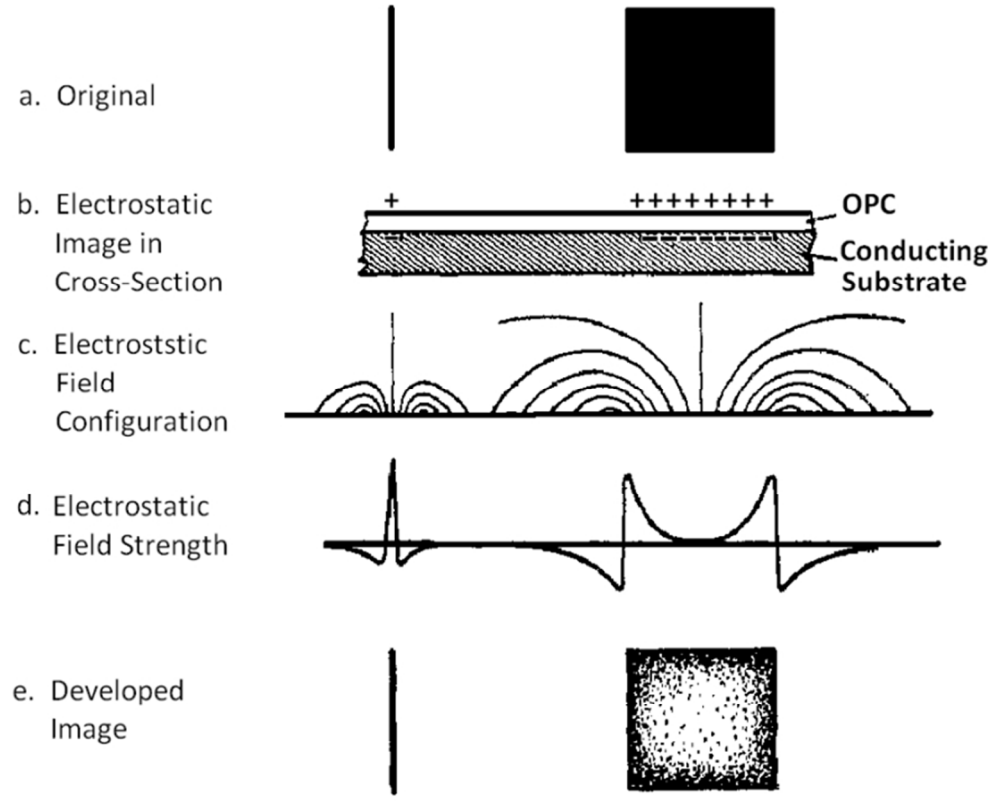
a. Original
b. Electrostatic Image in Cross-Section
+
++++++++
OPC
Conducting Substrate
c. Electroststic Field Configuration
d. Electrostatic Field Strength
e. Developed Image

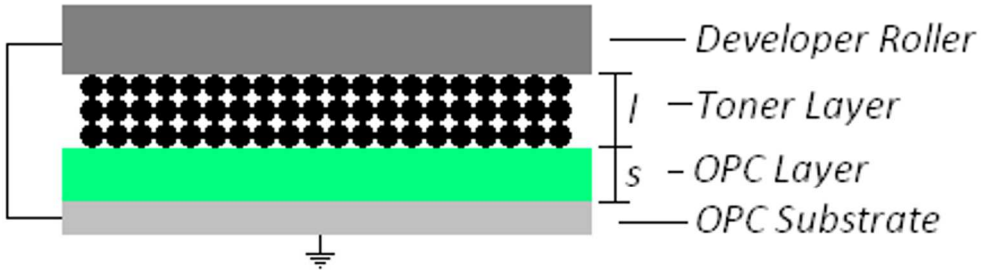

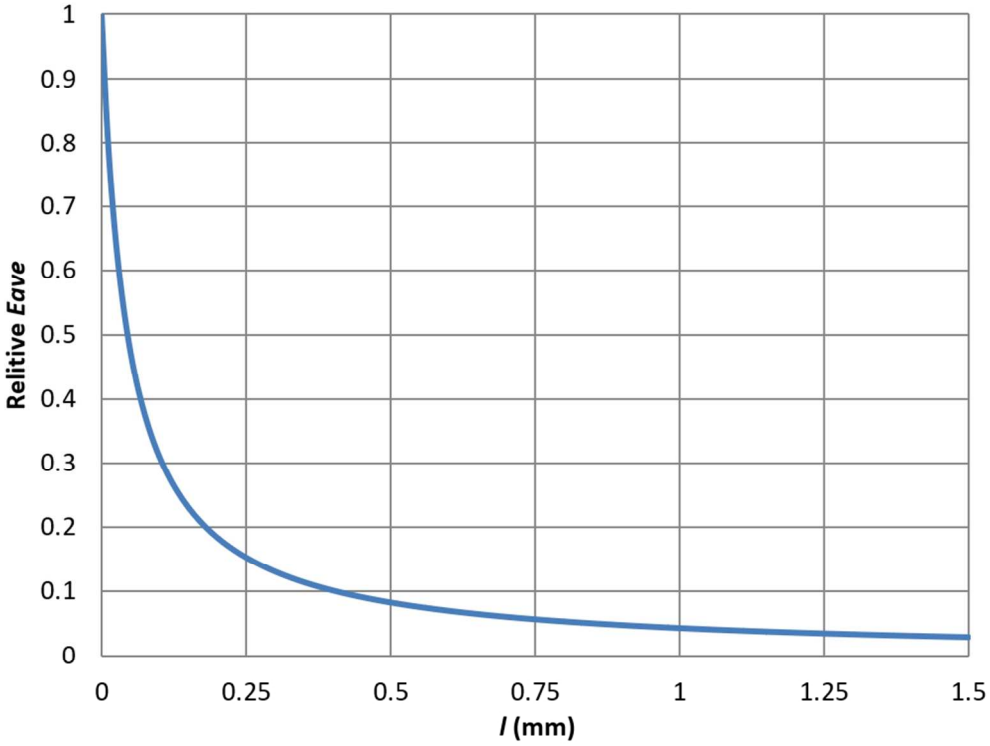
Relitive Eave
1
0.9
0.8
0.7
0.6
0.5
0.4
0.3
0.2
0.1
0
0
0.25
0.5
0.75
1
1.25
1.5
l (mm)

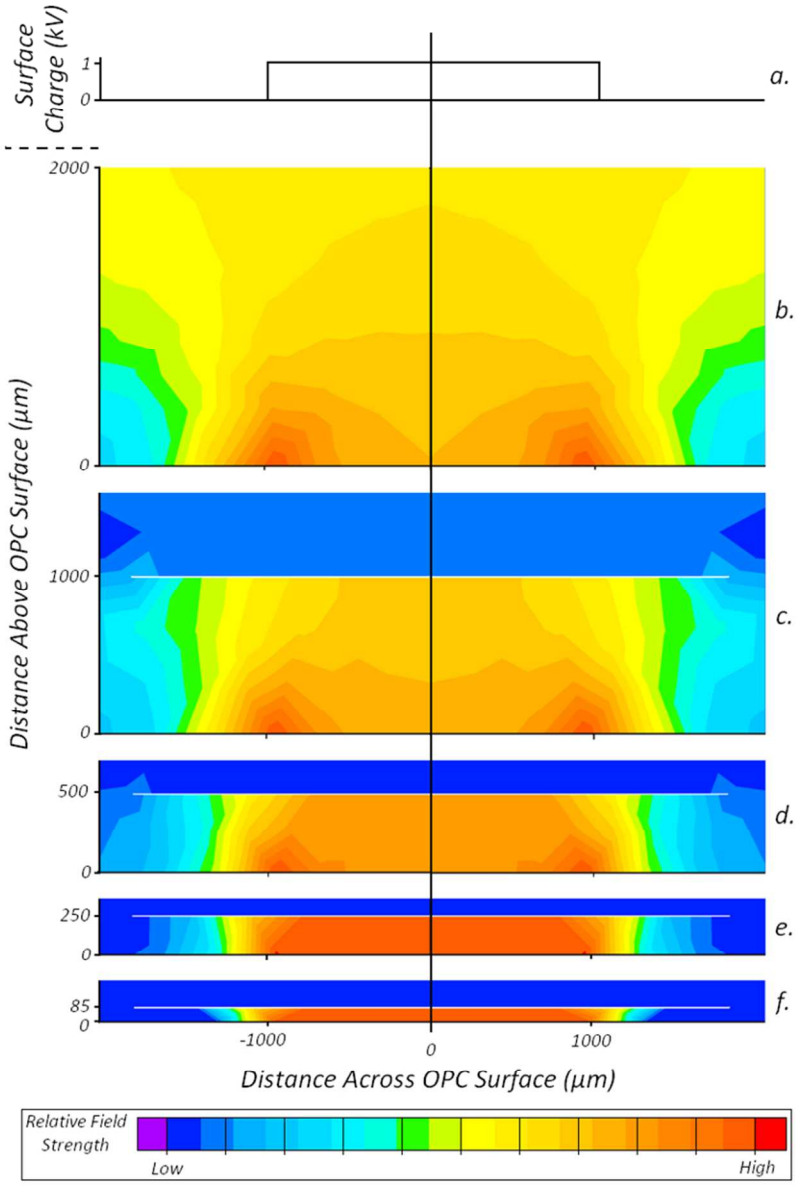
Surface Charge (kV)
1
0
a.
2000
0
b.
Distance Above OPC Surface (µm)
1000
0
c.
500
0
d.
250
0
e.
85
0
f.
-1000
0
1000
Distance Across OPC Surface (µm)
Relative Field Strength
Low
High